

Universal quantum computation with quantum-dot cellular automata in dephasing-free subspace

Z. Y. Xu^{1,2}, M. Feng^{1,*} and W. M. Zhang³

¹*State Key Laboratory of Magnetic Resonance and Atomic and Molecular Physics, Wuhan Institute of Physics and Mathematics, Chinese Academy of Sciences, Wuhan, 430071, China*

²*Graduate School of the Chinese Academy of Sciences, Beijing, 100049, China and*

³*Department of Physics and Center for Quantum Information Science, National Cheng Kung University, Tainan 70101, China*

We investigate the possibility to have electron-pairs in dephasing-free subspace (DFS), by means of the quantum-dot cellular automata (QCA) and single-spin rotations, to carry out a high-fidelity and deterministic universal quantum computation. We show that our QCA device with electrons tunneling two dimensionally is very suitable for DFS encoding, and argue that our design favors a scalable quantum computation robust to collective dephasing errors.

PACS numbers: 03.67.Pp, 73.63.-b, 03.67.Lx

Spin degrees of freedom of electrons in quantum dots have been considered as good candidates to encode qubits over past years, due to their long decoherence time and full controllability. Of particular interest is the recent achievements of ultrafast manipulation of electron spin in conduction band of the quantum dot [1, 2] and coherent tunneling of electrons between neighboring quantum dots [3, 4]. These technical progresses have led to more and more concerns on universal quantum computation (UQC) based on movable electrons.

It has been shown in [5, 6, 7, 8] that the independence between spin and charge degrees of freedom of the electrons results in the possibility of electrons performing UQC. The key idea is that we encode qubits in the electron spins, but make measurement [5, 6] or make entanglement [7, 8] by means of the electron charges. With these ideas, we could use the movable (or say, free) electrons to entangle the spin states of different electrons [5, 6, 7, 8, 9], to analyze the multipartite entanglement [5, 9], and to purify the existing entanglement [10].

However, the electron spins in quantum dots severely suffer from the surrounding nuclear spins [11, 12], and the confinement of the quantum dots makes the decoherence enhanced. Except some special cases [13], the interaction of the nuclear spins with the electronic spins is detrimental. Normally, we may introduce spin-echo techniques to counteract the collective dephasing by a reverse time evolution during some selected periods. But spin-echo does not work for the ambient magnetic fluctuations, such as from the thermally distributed nuclear spins. To reduce this dephasing, we have to employ dephasing-free subspace (DFS) which resists collective dephasing due to symmetric encoding [14, 15].

We focus in the present work on the recently proposed device, i.e., quantum-dot cellular automata (QCA), based on which entanglement of different electron spins could be achieved without spin-spin interaction [7, 8]. We will show that UQC could be carried out by QCA settings in a relatively simpler way than by other systems.

QCA was originally proposed as a transistorless alternative to digital circuit devices at the nanoscale [16]. When we apply it to quantum dots, QCA behaves quantum mechanically with two electrons tunneling coherently between two antipodal sites on the QCA due to Coulomb repulsion. So different from the free-electron QC models under screening assumption [5, 6], QCA makes deterministic operations using the Coulomb interaction between electrons [7, 8]. This unique quantum mechanical feature along with single-spin rotations could lead to deterministic spin-spin entanglement between electrons, which is applicable to UQC [8] and to generation of entangled photon pairs [17].

The DFS we employ is spanned by the encoding states $|0_L\rangle = |01\rangle$ and $|1_L\rangle = |10\rangle$ with $|0\rangle$ and $|1\rangle$ the spin up and down states of the electron in the dot, respectively. For clarity, we will call $|0_L\rangle$ ($|1_L\rangle$) logic qubit and $|0\rangle$ ($|1\rangle$) physical qubit. As there is no spin-spin coupling between the electrons, we have degeneracy between $|0_L\rangle$ and $|1_L\rangle$, implying that no noise from collective dephasing would affect the encoded subspace we employ. It also means that the dot-dot spacing in our design must be bigger than those in [4, 11, 12]. As collective errors due to coupling to environment are generally considered to be the main problem in solid-state system at low temperature, we assume throughout this work the collective dephasing to be dominant in our system. Other non-collective phase noises could also be removed by some additional operations, as shown later. We will demonstrate that three basic logic gates for a UQC could be carried out by our DFS-encoded electron spins, without any auxiliary spin qubit required. As dephasing is strongly suppressed and the QC is run strictly within the DFS, the entangled state generated in our design could be kept in high fidelity for a long time.

As shown in Fig. 1(a), the QCA blocks and the quantum dots encoding the qubits are arranged in alternate way in two dimensions, where the large spacing between the qubits, e.g., hundreds of nanometers or even

of the order of micrometer to make sure the spin-spin interaction negligible, is helpful for individual manipulation on the qubits. To have a UQC in DFS, we have to construct three logic-qubit gates. The first is the Hadamard gate $H_L : |0_L\rangle = |01\rangle_{ii'} \Rightarrow \frac{1}{\sqrt{2}}(|0_L\rangle + |1_L\rangle) = \frac{1}{\sqrt{2}}(|01\rangle_{ii'} + |10\rangle_{ii'})$, and $|1_L\rangle = |10\rangle_{ii'} \Rightarrow \frac{1}{\sqrt{2}}(|0_L\rangle - |1_L\rangle) = \frac{1}{\sqrt{2}}(|01\rangle_{ii'} - |10\rangle_{ii'})$. The second gate is for a single-logic-qubit rotation $Q_L(\theta)$, i.e., $a|0_L\rangle + b|1_L\rangle \Rightarrow a|0_L\rangle + be^{i\theta}|1_L\rangle$. The third one is the two-logic-qubit conditional gate. We will construct a controlled-phase flip (CPF) as an example, i.e., a phase π appearing as the prefactor of $|1_L 1_L\rangle$ after the gating. Consider the initial state of the two electrons in quantum dots i and j to be $|e_i e_j\rangle \otimes |S_i S_j\rangle$, where $|e_i e_j\rangle$ are charge states to be auxiliary, $|S_i S_j\rangle$ are spin states for qubit encoding, and j could be i' in the case of H_L gating or $i+1$ for achieving CPF. After the electrons tunnel to dots A and C, we switch off the channels between the dots i, j and the QCA, and then turn on the bias for the electron tunneling between the sites A and B, and between the sites C and D (See Fig. 1(b)). We may describe the quantum behavior on the QCA by following Hamiltonian in units of $\hbar = 1$ [8],

$$H_{QCA} = \frac{\omega_0}{2}(|+\rangle\langle+| - |-\rangle\langle-|) + \frac{\gamma}{2}(|+\rangle\langle-| + |-\rangle\langle+|), \quad (1)$$

where $|+\rangle = |e_i^B e_j^D\rangle$ and $|-\rangle = |e_i^A e_j^C\rangle$ are polarized charge states defined in [7, 8] and in Fig. 1(c). ω_0 represents the energy offset of the polarized states $|\pm\rangle$ from the balance of on-site potential, Coulomb repulsion and the external bias energy. γ accounts for the tunneling between these two polarized states.

To carry out the first gate H_L , we set ω_0 to be zero (i.e., a symmetric QCA) and start the tunneling from the state $|-\rangle \otimes |S_i S_{i'}\rangle$ where the subscripts correspond to the dots the electrons come from, and the electron with spin $|S_i\rangle(|S_{i'}\rangle)$ will tunnel between A(C) and B(D). During the electron tunneling on the QCA, we perform single-spin rotations U_{BD} and U_{AC} on the electronic states at the sites B, D and A, C. As the tunneling is coherent, these single-spin operations could be done simultaneously [8]. At $t = \pi/2\gamma$, we stop our operations on the QCA, and drive the electrons back to dots i and i' [8]. Then we get $|e_i e_{i'}\rangle \otimes \frac{1}{\sqrt{2}}(U_{AC} - iU_{BD})|S_i S_{i'}\rangle$, where $U_{AC} = R_x^A(\pi) \otimes R_x^C(3\pi)$ and $U_{BD} = R_z^B(3\pi) \otimes I^D$, with the superscripts for the sites where the electron is rotated, $R_k(\theta) = \exp(-i\theta\sigma_k/2)$, $k = x, y, z$, and I being an identity operator. It is easy to verify that above operations yield $H_L : a|0_L\rangle + b|1_L\rangle \Rightarrow \frac{1}{\sqrt{2}}[a(|0_L\rangle + |1_L\rangle) + b(|0_L\rangle - |1_L\rangle)]$, as shown in Fig. 2(a).

The third gate happens between pairs $i - i'$ and $(i + 1) - (i' + 1)$ of the initial state $(a|01\rangle_{i,i'} + b|10\rangle_{i,i'}) \otimes (c|01\rangle_{i+1,i'+1} + d|10\rangle_{i+1,i'+1})$. The CPF yields $ac|0101\rangle_{i,i',i+1,i'+1} + ad|0110\rangle_{i,i',i+1,i'+1} + bc|1001\rangle_{i,i',i+1,i'+1} - bd|1010\rangle_{i,i',i+1,i'+1}$, which is actually equivalent to a CPF on electrons i and $i + 1$ in

the top line (See Fig. 2(b)). To achieve such a CPF, we may employ the controlled-NOT (CNOT) gate in [8] sandwiched by two Hadamard gates on the target physical qubit. But we hope to accomplish the CPF directly to make our implementation simple. So under the Hamiltonian H_{QCA} with $\omega_0 = 0$ and the initial state $|-\rangle \otimes |S_i S_{i+1}\rangle$, we start the tunneling assisted with single-spin rotations. Like in above H_L gating, we stop the electron tunneling at $t = \pi/2\gamma$, and drive the electrons back to the dots i and $i + 1$. So we have $|e_i e_{i+1}\rangle \otimes \frac{1}{\sqrt{2}}(\bar{U}_{AC} - i\bar{U}_{BD})|S_i S_{i+1}\rangle$, with $\bar{U}_{AC} = R_z^A(\pi/2) \otimes R_z^C(\pi/2)$ and $\bar{U}_{BD} = R_z^B(3\pi/2) \otimes R_z^D(3\pi/2)$, which yields

$$|\varphi\rangle = \frac{1}{\sqrt{2}}|e_i e_{i+1}\rangle \otimes (1 - i) \begin{pmatrix} 1 & 0 & 0 & 0 \\ 0 & 1 & 0 & 0 \\ 0 & 0 & 1 & 0 \\ 0 & 0 & 0 & -1 \end{pmatrix} |S_i S_{i+1}\rangle. \quad (2)$$

If we neglect the additional global phase, we have fulfilled the CPF operation: $|S_i S_{i+1}\rangle \Rightarrow (-1)^{S_i S_{i+1}} |S_i S_{i+1}\rangle$ between the dots i and $i + 1$, with $S_i, S_{i+1} = 0, 1$. This physical-qubit CPF also implies the logic-qubit CPF between pairs $i - i'$ and $(i + 1) - (i' + 1)$, as shown in Fig. 2(b).

The second gate $Q_L(\theta)$ could be achieved by rotating one of the physical qubits. So different from the first and the third gates, the implementation of the second gate employs Faraday rotation [18], instead of the tunneling on QCA. We apply $\sigma_{(z)}^+$ polarized light on a certain dot in the bottom line. A phase $e^{i\delta_0}$ ($e^{i\delta_1}$) will be created if the electron spin of the dot is initially $|0\rangle$ ($|1\rangle$), due to virtual excitation of exciton including heavy (light) hole state [18]. As δ_0 is larger than δ_1 and both of them could be exactly controlled, we could achieve $Q_L(\theta)$ with $\theta = \delta_0 - \delta_1$.

With the three basic gates above, we could carry out a universal quantum gating with the electron pairs. However, in terms of DiVincenzo's criteria [19], a UQC also requires high-quality preparation of initial states and the efficient readout, besides the universal quantum gating. In our case, the initial qubit states on the top line should be in $|00\dots 0\rangle$ (i.e., all spins up) and the qubit states on the bottom line are initially $|11\dots 1\rangle$ (i.e., all spins down), which correspond to the logic state $|0_L\rangle$. As the inter-dot separation is big, this job could be accomplished individually by the techniques in [1, 20], where a single conduction band electron was produced [20] and single-spin manipulation on the conduction band electron has been achieved [1]. The single-spin rotation could also be made by ultrafast laser pulses which accomplish substantial and accurate spin rotation at the timescale of femtosecond [2]. The efficient readout of qubit states has been available optically by nondestructive detection of the electron spin in the conduction band of the quantum dot [21]. The same job could also be done by single-shot

technique [22] based on the charge signal due to electron jumping. If the electron could jump back to the original site after the detection, this readout is also nondestructive [8]. Therefore, up to now, we have proved that a UQC with the DFS encoded electron pairs is available in our QCA-based device.

As it strongly suppresses the collective dephasing, the DFS encoding could much reduce the operations for spin-echo and thereby actually reduce the gating time and enhance the fidelity, although it seems to have the resource overhead increased. Besides collective dephasing, however, there would be other dephasing errors in a real system, such as logic errors and leakage errors [23]. To fully eliminate them, we have to employ 'Bang-Bang' control pulse sequences on the logic qubits, assisted sometimes by individual operations on the physical qubits [23]. All these operations could be done easily in our design. This implies that dephasing errors could be completely eliminated in our scheme. So T_2 in our design is in principle infinitely long. For other sources of decoherence beyond dephasing, the mechanism is very complicated, regarding background charge fluctuation and noise, electron-phonon interaction, low-frequency noise and so on [12]. For example, T_1 was reported to be of the order of hundreds of nanosec in a system of two-dimensional electron gas [8, 17], and in a preliminary experiment for QCA with two electrons involving no spin [24], the coherent tunneling of the electrons diminished very quickly. Although we have not yet fully understood these decoherence sources, lower temperature is helpful for suppressing most of them. We have also noticed that elaborately controlled spin-echo pulses could extend T_1 to 1 microsec [4]. As there is no fluctuation regarding spin-spin exchange energy and hybridized states [12] in our design due to negligible inter-spin coupling, we may expect T_1 in our design to be longer than tens of microsecond in the low temperature.

Using the values in [17], we may assess an entangled state between the electrons i and j to be achievable within 70 picosec, provided that the electron tunneling rate on the QCA could be as fast as 200 GHz [17]. As the implementation time is much shorter than T_1 , we may neglect decoherence in our discussion. But due to the rapid operation, we have to pay attention to the possible imprecision in the single-spin rotation and in the bias voltage control. For an estimate, we have assumed in our numerical calculation a laser induced phase error ϵ for every $\pi/2$ single-spin rotation and a phase error δ by voltage control in each tunneling on the QCA. Fig. 3 demonstrates the fidelity of H_L and CPF on different states under these errors. We could find that the error ϵ is more destructive than δ , which implies the accurate manipulation by laser to be more essential to our implementation. Another point is that the CPF works better than H_L under the same condition. The reason is that H_L involves larger rotations which bring about more phase

errors regarding ϵ . The results remind us to pay more attention to the operations by the ultrafast laser pulses.

Compared with previous devices producing entanglement between free electrons [5, 6, 9], our QCA-based design could achieve the logic-qubit quantum gates more straightforwardly in a simpler fashion. For example, the CPF gating could be made with much reduced steps compared to [5, 6, 9]. This is because that the free electrons under screening model [5, 6, 9] interact only by measurement, which is probabilistic, while our implementation, under Coulomb interaction, is made straightforwardly and deterministically. In addition, the measurement in [5, 6, 9] is made by the time-resolved charge detector which is technically unavailable at present, whereas no charge detector is required in our design. More importantly, as dephasing errors are strongly suppressed, the entangled states in our design, only restricted by T_1 , could be kept in high-fidelity for a longer time than in any proposal without using DFS.

To some extents, our scheme is similar to that with multizone trap by moving ions [15]. Both the electrons in our design and the ultracold ions in the trap are exactly controllable, e.g., to be static and moving under control. Besides, both the designs are scalable, and deterministically operated. It has been shown in [15] that the DFS encoding could suppress the collective dephasing errors in trapped ions separated by $5 \sim 10 \mu\text{m}$ to 10^{-4} . So it should work better in our design with the dots' spacing approximately $1 \mu\text{m}$. On the other hand, due to controllable tunneling in a two-dimensional configuration, our designed QCA setting is more favorable for UQC in DFS than ion traps or other systems: We need no movement of qubits for a long distance as in multizone trap [15], and the dephasing resisted UQC could be achieved with no need of auxiliary qubits [25] and no danger going beyond the DFS during operation [26]. What is more, the above proposals [25, 26] are probabilistic due to measurement involved, whereas our implementation is deterministic.

In summary, we have demonstrated the possibility to carry out a UQC robust to dephasing errors by a QCA-based device using electronic tunneling and single-spin rotations. Our scheme only involves gate voltage controls of the electron tunneling and optical manipulation of the electron spin in quantum dots. Although some of the necessary steps are still challenging with current experimental techniques, our proposed design without spin-spin interaction and dephasing errors, but with relatively large dot-dot spacing, is helpful for experimental observation of coherence and entanglement of electron spins in quantum dots and provides a promising way toward scalable QC with quantum dots.

This work is partly supported by NNSF of China under Grant No. 10774163, and partly by the NFRP of China under Grants No. 2005CB724502 and No. 2006CB921203.

* Electronic address: mangfeng@wipm.ac.cn

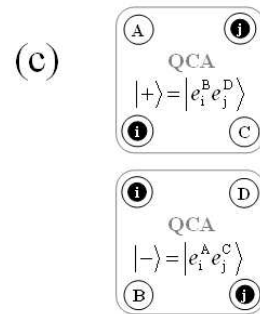
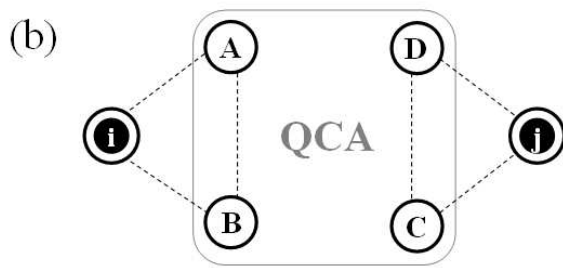
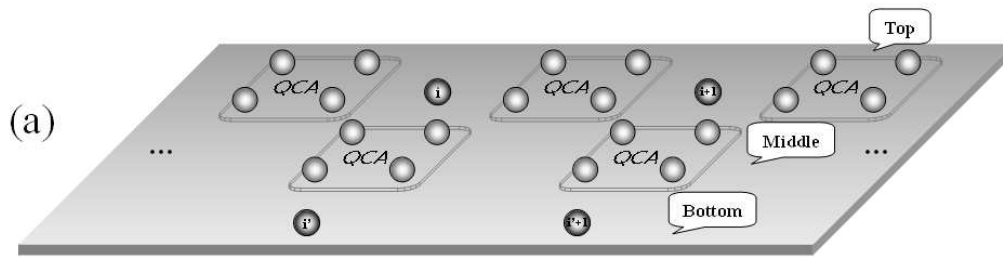
- [1] Kroutvar *et al*, Nature (London) **432**, 81 (2004).
 [2] J. A. Gupta, R. Knobel, N. Samarth, and D. D. Awschalom, Science **292**, 2458 (2001).
 [3] T. Hayashi *et al*, Phys. Rev. Lett. **91**, 226804 (2003).
 [4] J. R. Petta *et al*, Science **309** 2180 (2007).
 [5] C. W. J. Beenakker *et al*, Phys. Rev. Lett. **93**, 020501 (2004).
 [6] H. A. Engle and D. Loss, Science **309**, 586 (2005).
 [7] Y. Z. Wu and W. M. Zhang, Europhys. Lett. **71**, 524 (2005).
 [8] W. M. Zhang, Y. Z. Wu, C. Soo and M. Feng, Phys. Rev. B **76**, 165311 (2007).
 [9] X. L. Zhang, M. Feng, and K. L. Gao, Phys. Rev. A **73**, 014301 (2006).
 [10] X. L. Feng, L.C. Kwek, and C.H. Oh, Phys. Rev. A **71**, 064301 (2005).
 [11] D. Klauser, W. A. Coish and D. Loss, Phys. Rev. B **73**, 205302 (2006).
 [12] A. Romito and Y. Gefen, Phys. Rev. B **76**, 195318 (2007).
 [13] A. Greilich *et al*, Science **317**, 1896 (2007).
 [14] A. Beige, D. Braun, and P. L. Knight, New J. Phys. **2**, 22 (2000); Paul G. Kwiat *et al*, Science **290**, 498 (2000).
 [15] M. Feng, Phys. Rev. A **63**, 052308 (2001); D. Kielpinski *et al*, Science **291**, 1013 (2001); D. Kielpinski, C. Monroe, and D. J. Wineland, Nature (London) **417**, 709 (2002).
 [16] A. O. Orlov *et al*, Science **277** 928 (1997); Orlov A O *et al*, Appl. Phys. Lett. **74** 2875 (1999).
 [17] M. Feng, J. H. An and W. M. Zhang, J. Phys. C **19**, 326215 (2007).
 [18] F. Meier and B. P. Zakharchenya, *Optical Orientation*, (Elsevier, Amsterdam, 1984).
 [19] D. P. DiVincenzo, Forsch. Phys. **48**, 9, (2000).
 [20] J. J. Finley *et al*, Appl. Phys. Lett. **73**, 2618 (1998).
 [21] J. Berezovsky *et al*, Science **314**, 1916 (2006).
 [22] J. M. Elzerman *et al*, Nature (London) **430**, 431 (2004).
 [23] M. S. Byrd and D. A. Lidar, Phys. Rev. Lett. **89**, 047901 (2002); L. -A. Wu, M. S. Byrd and D. A. Lidar, Phys. Rev. Lett. **89**, 127901 (2002).
 [24] S. Gardelis *et al*, Phys. Rev. B **67** 033302 (2003).
 [25] P. Xue and Y. F. Xiao, Phys. Rev. Lett. **97**, 140501 (2006).
 [26] Z. J. Deng, M. Feng, and K. L. Gao, Phys. Rev. A **75**, 024302 (2007).

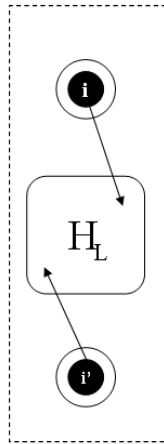
Figure Captions

Fig. 1 (a) Schematics for our proposed design, where the dots i , with $i = 1, 2, 3, \dots$, are initially prepared in $|0\rangle$, and dots i' , with $i' = 1', 2', 3', \dots$, are initially in $|1\rangle$. The logic qubits are constructed by $|i\rangle_{i'}$. (b) Four initially neutral quantum dots in the square constitute a QCA, and two initially charged quantum dots are separated by the QCA, where the black dots represent single electrons and the dashed lines connecting quantum dots denote possible tunnelings. (c) Coulomb repulsion causes two full polarized charge states $|+\rangle = |e_i^B e_j^D\rangle$ and $|-\rangle = |e_i^A e_j^C\rangle$, where A, B, C and D mean the sites and i and j denote the different electron spins.

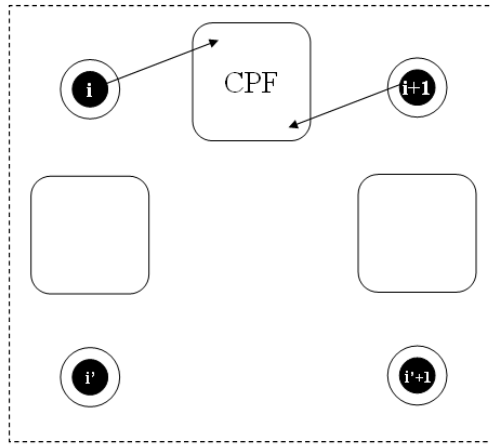
Fig. 2 Logic-qubit quantum gates, where (a) is for H_L carried out between dots i and i' . (b) is for CPF between dots i and $i + 1$ in the top line.

Fig. 3 (Color online) Numerical simulation for the fidelity of the gating H_L and CPF under imprecise operations, where ϵ and δ are phase errors induced, respectively, in the laser manipulation and the voltage control. The curved surfaces in red and yellow represent H_L on logic-qubits $|0_L\rangle$ and $|1_L\rangle$, respectively, and the blue surface is for CPF on the state $|\Phi\rangle = (|00\rangle + |01\rangle + |10\rangle + |11\rangle)/2$.





(a)



(b)